

Design, Synthesis, and Biological Evaluation of 1-[(2-Benzyloxy/alkoxy)methyl]-5-halo-6-arylluracils as Potent HIV-1 Non-nucleoside Reverse Transcriptase Inhibitors with an Improved Drug Resistance Profile

Xiaowei Wang,^{†,#} Jianfang Zhang,^{†,#} Yang Huang,^{§,#} Ruiping Wang,[†] Liang Zhang,[†] Kang Qiao,[†] Li Li,[†] Chang Liu,[†] Yabo Ouyang,[§] Weisi Xu,[§] Zhili Zhang,[†] Liangren Zhang,[‡] Yiming Shao,[§] Shibo Jiang,[¶] Liying Ma,^{*,§} and Junyi Liu^{*,†,‡}

[†]Department of Chemical Biology, School of Pharmaceutical Sciences; [‡]State Key Laboratory of Natural and Biomimetic Drugs, Peking University, Beijing 100191;

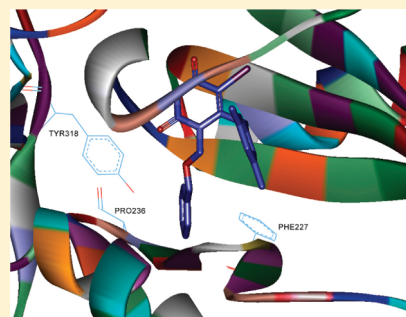
[§]State Key Laboratory for Infection Disease Prevention and Control, National Center for AIDS/STD Control and Prevention (NCAIDS), Chinese Center for Disease Control and Prevention, Beijing 102206

[†]College of Pharmaceutical Sciences, Capital Medical University, Beijing 100069

[¶]MOE/MOH Key Laboratory of Medical Molecular Virology, Shanghai Medical College and Institute of Medical Microbiology, Fudan University, Shanghai 200032, China

Supporting Information

ABSTRACT: Because the emergence of drug-resistant mutants has limited the efficacy of non-nucleoside reverse transcriptase inhibitors (NNRTIs), it is essential to develop new antivirals with better drug resistance and pharmacokinetic profiles. Here we designed and synthesized a series of 1-[(2-benzyloxy/alkoxy)methyl]-5-halo-6-arylluracils, the HEPT analogues, and evaluated their biological activity using nevirapine and **18** (TNK-651) as reference compounds. Most of these compounds, especially **6b**, **7b**, **9b**, **11b**, and **7c**, exhibited highly potent anti-HIV-1 activity against both wild-type and NNRTI-resistant HIV-1 strains. Compound **7b**, which had the highest selectivity index (SI = 38 215), is more potent than nevirapine and **18**. These results suggest that the introduction of a halogen at the C-5 position may contribute to the effectiveness of these compounds against RTI-resistant variants. In addition, meta substituents on the C-6 aromatic moiety could significantly enhance activity against NNRTI-resistant HIV-1 strains. These compounds can be further developed as next-generation NNRTIs with an improved antiviral efficacy and drug-resistance profile.



INTRODUCTION

Reverse transcriptase (RT) of human immunodeficiency virus type 1 (HIV-1) is an attractive target for development of drugs used in the treatment of HIV-1 infection and AIDS. It is a multifunctional enzyme critical in viral replication. Currently, two functionally distinct classes of HIV-1 RT inhibitors (nucleoside and non-nucleoside) have been discovered and are being used clinically. Especially, non-nucleoside RT inhibitors (NNRTIs), with a wide range of chemically diverse structures, have gained a definitive and important place in clinical use based on their unique antiviral potency with generally low toxicity and favorable pharmacokinetic properties.^{1–3} To date, four NNRTIs have been approved for clinical use: nevirapine, delavirdine, efavirenz, and etravirine.^{4–9}

Crystal structures of several RT/NNRTI complexes clearly show that NNRTIs bind to a hydrophobic pocket (the non-nucleoside inhibitor binding pocket, NNIBP) in the p66 palm subdomain near the polymerase active site. Upon binding, NNRTIs cause a distortion of the catalytic aspartate site.^{10–12}

Like other types of anti-HIV drugs, the therapeutic efficacy of NNRTIs has been limited by the emergence of mutants that show cross-resistance to other structurally unrelated drugs.^{13–17} Therefore, it is essential to develop new NNRTIs with improved pharmacokinetic and drug-resistance profiles.

Among more than 50 different series of NNRTIs that have been reported so far, 1-[(2-hydroxyethoxy) methyl]-6-(phenylthio)thymine (HEPT) was the first compound shown to target specifically HIV-1 RT.¹⁸ Here we designed and synthesized 22 HEPT (16) derivatives and detected their inhibitory activity on HIV-1 RT activity. Then, we selected 11 active compounds for testing of antiviral activities against HIV-1_{SF33}, a laboratory-adapted HIV-1 X4/R5 dual tropic strain, and HIV-1_{A17}, an NNRTI-resistant variant. On the basis of the results, we will delineate their structural features and gain insight into how the major chemical substitutions on the

Received: November 7, 2011

Published: January 27, 2012



pyrimidine backbone affect the activity of these inhibitors against NNRTI-resistant HIV-1 strains.

MOLECULAR DESIGN

Structure–activity relationship studies have developed promising **16** analogues such as **17** (MKC-442) and **18** (TNK-651)^{19–21} (Figure 1), and the substituent on C-5 and C-6 of

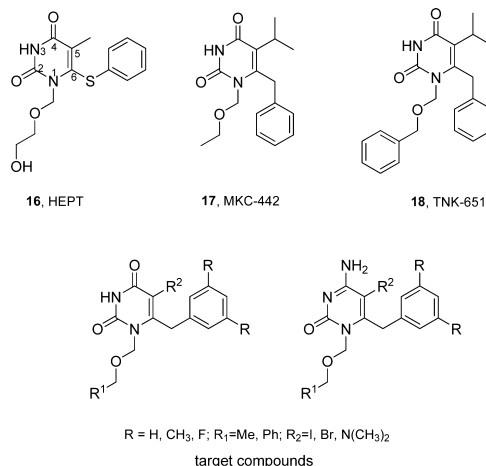


Figure 1. Structure of **16** analogues and target compounds.

the pyrimidine ring has been revealed as very important for antiviral activity.^{22,23} Interestingly, **17** and **18**, with their bulky isopropyl groups at the C-5 position, have been shown to counteract the Tyr181 residue,²⁴ thus forcing it into a position where strong interaction with the 6-benzyl group of the inhibitor can take place. In contrast, the C-5 methyl group in **16** does not produce any “trigger effect” but only brings a slight perturbation of the Tyr181 side-chain conformation.

Although considerable research has been performed to understand the structure–activity relationship of **16** analogues, little information can be found to explain the effect of varying both electronic effect and steric hindrance of the **16** series at the C-5 position with a halogen. Compared to **18**, for example, the C-5 halogen atom has a large electron cloud density, which could form an interaction with the binding site of RT and play an important role in improving anti-HIV-1 activity. Moreover, the large atomic radius of the C-5 halogen may also provide a steric hindrance role, when compared with the C-5 isopropyl of **18**, and could trigger the conformation of a C-6 aromatic ring. In addition, modification to the C-6 by introduction of a *m*-dimethyl- or *m*-difluorophenyl moiety onto the phenylmethyl

ring may result in closer interactions with the non-nucleoside binding pocket (NNBP) than can be achieved with **18**.

To investigate the role of hydrogen bonds, we designed and synthesized a series of compounds by exchanging C-4-OH for -NH₂, expecting that two hydrogen bonds could be formed between the N-3/C-4 positions with the carbonyl group of Lys101. Computational studies on the possible binding mode of these **16** derivatives in the NNBP of HIV-1 RT suggest that the introduction of a further anchor, which acts as both donor and acceptor of hydrogen bonds, would potentially lead to more activity against HIV-1 viruses.²⁵

To verify the structure–activity relationship of our design, target compounds 1-[(2-benzoyloxy)methyl]-5-iodo-6-aryluracils (**7a**, **7b**, and **7c**) were flexibly docked into the binding site of HIV-1 RT (PDB entry 1RT2, complexes with **18**), using the GOLD3.0.1 docking program. It was revealed that the binding mode of **7a**, **7b**, and **7c** has approximate conformations comparable to that of the RT/**18** complex (Figure 2).

On the basis of the above results, we then synthesized a series of novel uracil derivatives (Figure 1), which are characterized by methyl and fluorine at the meta positions of the phenyl ring, and all possess a halo or dimethylamino moiety at position 5 of the pyrimidine. Title compounds were tested for their activities against HIV-1 in both cell-based assay and reverse transcriptase (RT) assay in comparison with **18** and nevirapine, which were used as reference drugs. The results are described below.

CHEMISTRY

A conventional strategy of synthesizing the newly designed compounds is described in Scheme 1. We prepared the 3-oxo esters **1a–c** according to the method of Hannick and Kishi²⁶ by reaction of 2-bromoacetate with phenylacetonitrile or 3,5-dimethylphenylacetonitrile or 3,5-difluorophenyl acetonitrile, respectively. The β -ketoesters (**1**) were then converted by reaction with thiourea and sodium in ethanol into 2-thiouracils (**2**),²⁷ which were refluxed with 10% chloroacetic acid to yield 6-(arylmethyl)uracils (**3**).²⁸ Halogenations at the C-5 position of **3** by reaction of PbO₂ with halogen in glacial acetic acid at room temperature led to **4a–5b** in high yield. Compounds **4a–5b** were silylated in situ with *N,O*-bis(trimethylsilyl)acetamide (BSA) and then N-1 alkylated with the appropriate alkyl chloromethyl ether, in the presence of LiI, to give **6a–9b**^{29,30} in good yield, followed by reaction with aqueous dimethylamino solution to get **10a–11b**.^{31,32} Finally, the uracil moiety was successfully converted to the 4-(1,2,4-triazolyl)pyrimidinone derivatives. Without purification, subsequent ammonia treatment yielded the target compounds **12a–15b**.^{33–35} Structure

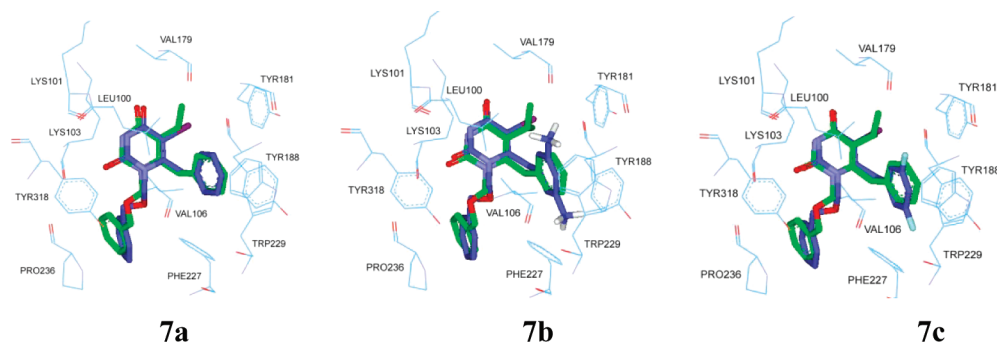
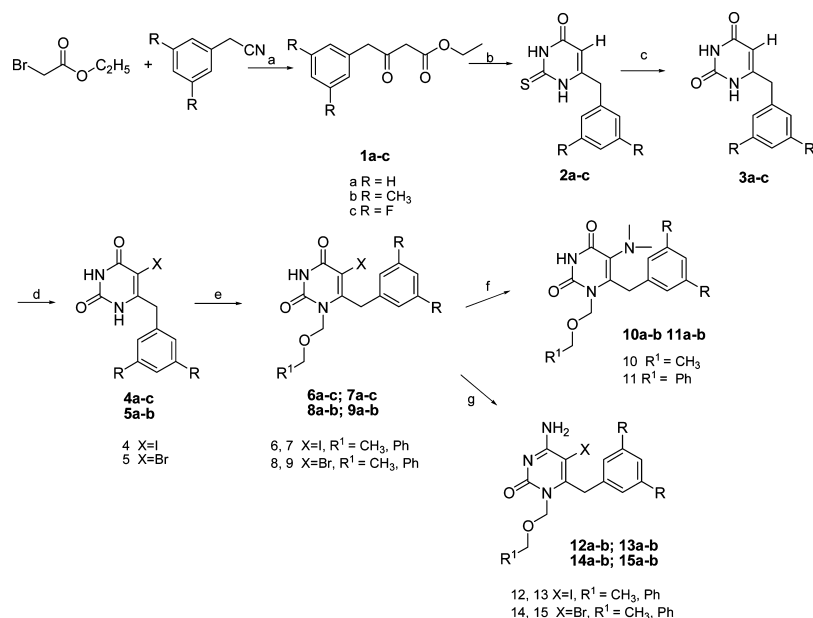


Figure 2. Superimposed stereoview of the docked **7a**, **7b**, and **7c**, (blue) with **18** (green).

Scheme 1^a

^aReagents and conditions: (a) aryl acetonitrile, Zn/THF, reflux; (b) thiourea, EtONa, EtOH, reflux; (c) 10% ClCH₂COOH, reflux; (d) halogen, PbO₂, glacial acetic acid; (e) alkyl halide, BSA, LiI, rt; (f) aq NH(CH₃)₂ solution, 60–80 °C; (g) POCl₃, 1,2,4-*H*-triazole, TEA, NH₃·H₂O, dioxane.

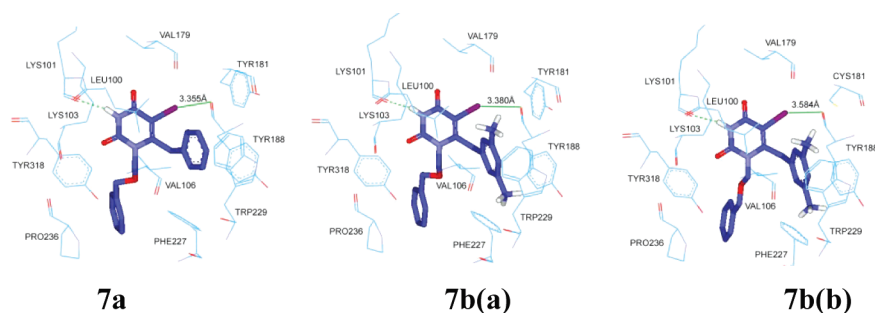


Figure 3. Docking results of **7a** into the 1RT2 NNBP, and **7b** into the NNBP of 1RT2 (a) and 1JLA Tyr181Cys (b). Hydrogen bonds are shown as a green dashed line, and halogen bonds are shown as a green solid line.

assignments of these compounds were identified by NMR and mass spectral data.

RESULTS AND DISCUSSION

Docking studies of the title compounds into the HIV-1 NNBP revealed that they could bind to the NNBP and displayed a slightly different binding mode compared to HIV-1 RT/18 complex. In particular, the C-5-isopropyl group of **18**, which is responsible for the “trigger action”, does not coincide with the halogen on the C-5 position of compounds **6a–9b**. Moreover, the disubstitution on the phenyl rings of **7b** and **7c** is at different positions comparing to that of **18** (Figure 2).

Within the NNBP, target compounds establish several ligand–receptor interactions. Inspection of the **7a**/RT complex (Figure 3) may be characterized as follows: (i) A hydrogen bond donated by the 3-NH function of the pyrimidine to the carbonyl oxygen of Lys101 is a crucial factor for anti-HIV-1 activity. (ii) Unusual interactions between the iodine atom and an electronegative atom, such as the Tyr188 carbonyl oxygen, were observed in the **7a** /RT structure. Here, demonstrating electrostatic dynamics, the iodine atom serves as an electron acceptor for the Tyr188 carbonyl oxygen (Figure 3). The results suggested that halogen, especially iodine on the

pyrimidine ring, has anisotropic surface charge distributions with significant electropositive patches which could serve as a Lewis acid. Thus, the introduction of electron-withdrawing substituents on the pyrimidine ring might increase the electrostatic interaction of the compound with the carbonyl oxygen of Tyr188 residue. In addition, the iodine atom of **7a** is only 3.35 Å away from the carbonyl oxygen of Tyr188, which is less than the van der Waals contact distance of 3.55 Å, and the angle C–X···O (X is a halogen) of **7a** is 157.93°, which is close to the predicted ideal angle of 165°. (iii) Favorable π -stacking interactions of the **7a** phenyl ring with a hydrophobic pocket, as defined by the side chains of Tyr188, Trp229, Tyr181, Leu100, and Phe227, especially the Tyr188 and Tyr181 residues, were observed.

Interestingly, the antiviral results show that the chain at the C-6 position with different substituents on the aromatic moiety, which is located in a hydrophobic region delimited by Tyr181, Tyr188, Phe227, and Trp229, significantly enhances the activity against HIV-1 and demonstrates improved resistance profiles. We have investigated **7b**, **9b**, and **11b** by introduction of *m*-dimethyl substitution onto the phenyl ring intended to optimize interactions with Trp229, which is less mutable in immunodeficiency virus reverse transcriptase, by reducing the

dependence on binding to Tyr181. Molecular modeling revealed that methyl groups attached to the 3' and 5' positions of the 6-benzyl group would be buried in a deep hydrophobic region near Trp229 and Phe227 (Figure 3).

The significant difference in behavior of **7b** against the drug-resistant mutants is fully explained by the presence of the additional *m*-methyl groups, sitting comfortably in a deep hydrophobic region of the NNRTI binding site and, hence, increasing the van der Waals contacts and σ - π interactions to the conserved Trp229 and Phe227, as well as the other residues in this region. As a result, the compound derives a fraction of its binding energy from the interaction with the Tyr181 side chain.

Furthermore, the phenyl moiety at the terminus of the N-1 side chain extends into a tunnel that leads out of the NNIBP toward the catalytic site composed of Tyr318 and Pro236 (Figure 4). Particularly, Tyr318 could provide the π - π

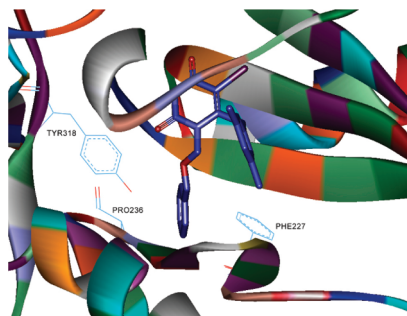


Figure 4. Docking results of **7b** into the 1RT2 NNBP.

interaction with the phenyl ring of the N-1 group. We presume that the steric hindrance aroused by the dimethyl substitution in **7b** would change the conformation of the ligand binding model in NNIBP with the rotation of the terminal phenyl moiety at the N-1 side chain and result in significantly improving the inhibition of HIV-1 RT, suggesting that

structure-based modifications at this location might enhance the activity.

Replacement of the dimethyl substitution in **7b** by difluoro substitution (**7c**), at the C-6-substituted aromatic ring, could also result in high potency against wild HIV-1 and Tyr181Cys mutant virus. This finding could be explained by a putative π -stacking interaction which would be improved between the electron-deficient benzene ring of the ligand and the electron-rich benzene ring of Tyr188, through introduction of the 3,5-difluorophenylmethyl moiety onto the C-6 position of the aromatic ring. Moreover, the contact distance between the iodine atom of **7c** and the carbonyl oxygen of Tyr188 is 3.27 Å, within the van der Waals distance, and the halogen bonding angle ((C-X...O), 155.44°) is similar to the ideal angle 165°.

Upon replacement of the C-4-OH by -NH₂, the binding mode changed such that the distance between the iodine with the carbonyl oxygen of Tyr188 (4.85 Å) became longer than the van der Waals distance (3.55 Å). Furthermore, the π -stacking interaction, which is usually present in our target compounds, was not observed in compound **13a**.

The title compounds were tested for their inhibitory activity against HIV-1 RT using a poly(ra)/oligo(dT)15 homopolymer template and nevirapine as a reference compound.³⁶ As shown in Table 1, nine compounds showed promising anti-RT activities. Particularly, compound **7b** is 1373- and 6.7-fold more potent than nevirapine and **18**, respectively. However, the anti-RT activities of compounds **12a**–**15b** significantly decreased.

Subsequently, the anti-HIV-1 activity and cytotoxicity of **6a**–**11b** were determined, using nevirapine and **18** as reference compounds. As shown in Table 2, all these compounds were capable of inhibiting infection by HIV-1_{SF33} in MT4 cells with EC₅₀ values ranging from 2 nM to 2.071 μM. Among these compounds, **7b**, **11b**, **9b**, **6b**, and **7c** were about 325- to 46-fold more potent than nevirapine. They had a higher antiviral activity and selectivity index (SI) than that of **18**. In addition, the above-mentioned compounds displayed much higher potency against HIV-1_{A17}, the NNRTI-resistant mutant strain

Table 1. Inhibitory Activity of the Target Compounds against HIV-1 RT (**6a**–**15b**)

compd	-C-4	R	R ¹	R ²	IC ₅₀ ^a	compd	C-4	R	R ¹	R ²	IC ₅₀ ^a
6b	O	3,5-dimethyl	Me	I	0.110	6a	O	H	Me	I	0.114
7b	O	3,5-dimethyl	Ph	I	0.003	7a	O	H	Ph	I	0.010
8b	O	3,5-dimethyl	Me	Br	0.210	8a	O	H	Me	Br	1.825
9b	O	3,5-dimethyl	Ph	Br	0.043	9a	O	H	Ph	Br	1.521
10b	O	3,5-dimethyl	Me	N(CH ₃) ₂	0.039	10a	O	H	Me	N(CH ₃) ₂	0.162
11b	O	3,5-dimethyl	Ph	N(CH ₃) ₂	0.021	11a	O	H	Ph	N(CH ₃) ₂	0.012
12b	NH ₂	3,5-dimethyl	Me	I	>100	12a	NH ₂	H	Me	I	>100
13b	NH ₂	3,5-dimethyl	Ph	I	7.217	13a	NH ₂	H	Ph	I	>100
14b	NH ₂	3,5-dimethyl	Me	Br	>100	14a	NH ₂	H	Me	Br	>100
15b	NH ₂	3,5-dimethyl	Ph	Br	16.338	15a	NH ₂	H	Ph	Br	>100
NVP ^b					4.120	6c	O	F	Me	I	11.85
17					0.150	7c	O	F	Ph	I	0.015
18					0.020						

^aEffective dose (μM) of the compounds required to inhibit HIV-1 RT activity by 50%. ^bNevirapine (NVP), **17**, and **18** were used as the reference compounds.

Table 2. Inhibitory Activity of the Compounds on HIV-1_{SF33} and HIV-1_{A17} Infection in MT4 Cells^a

compd	MW	CC ₅₀ (μM)	inhibition: EC ₅₀ (μM)		SI ^b	
			HIV-1 _{SF33}	HIV-1 _{A17}	HIV-1 _{SF33}	HIV-1 _{A17}
7a	448	74.84 ± 1.67	0.045 ± 0.014	>10	1663	<7
11a	365	91.82 ± 4.01	0.345 ± 0.134	>10	264	<9
10a	303	166.34 ± 8.75	0.614 ± 0.423	>10	270	<16.6
9a	401	67.36 ± 8.01	1.720 ± 0.962	>10	39	<6.7
8a	339	155.27 ± 6.05	2.071 ± 1.321	>10	75	<15.5
7b	476	98.31 ± 2.66	0.002 ± 0.001	0.091 ± 0.039	38215	1080
11b	393	55.81 ± 2.19	0.014 ± 0.009	2.198 ± 0.445	5201	25
9b	429	152.18 ± 9.60	0.009 ± 0.006	0.601 ± 0.270	16889	253
6b	414	141.52 ± 1.86	0.006 ± 0.005	0.637 ± 0.145	23667	222
6c	422	300.00 ± 9.21	0.537 ± 0.243	>10	559	<30
7c	484	121.25 ± 4.27	0.006 ± 0.002	2.543 ± 0.404	20208	48
NVP ^b	111	325.13 ± 0.02	0.068 ± 0.230	>10	4781	<35
18	302	84.60 ± 3.25	0.022 ± 0.015	>10	3845	<6.6

^aEach compound was tested in triplicate; the data were presented as the mean ± SD. ^bSI was calculated based on the CC₅₀ for MT4 cells and EC₅₀ for inhibiting infection by HIV-1_{SF33} and HIV-1_{A17}, respectively. Nevirapine (NVP) and 18 were used as the reference compounds.

with K103N and Y181C mutations, than that of nevirapine and 18.

CONCLUSION

In summary, we have designed a series of 1-[(benzyloxy/alkoxy)methyl]-5-halo-6-aryl uracil and 1-[(benzyloxy/alkoxy)methyl]-4-amino-5-halo-6-aryl uracil (**6a–15b**) as inhibitors of HIV-1 RT and described an efficient method of synthesis. Interestingly, compounds **7a–c**, **9a,b**, and **11a,b** showed antiviral activities much more potent than those of nevirapine, both in enzyme and cell-based assays. An excellent correlation was found between EC₅₀ values for inhibiting HIV-1 infection and IC₅₀ values for inhibiting HIV-1 RT activity, confirming that these compounds act as inhibitors of the HIV-1 RT.

Some of the dimethyl-substituted compounds (**6b**, **7b**, **9b**, and **11b**) had antiviral activity against wild-type HIV-1 comparable to that of 18. However, they were more effective than 18 against the NNRTI-resistant HIV-1 strain A17. This may have resulted from the introduction of two methyl groups to the C-6-substituted aromatic ring, which could increase contacts to the conserved Trp229 and modulate the terminal phenyl moiety at the N-1 side chain.

Meanwhile, the difluoro-substituted derivative (compound **7c**) showed a significant anti-HIV-1 potency for HIV-1_{SF33} and HIV-1_{A17} infection in MT4 cells, compared to that of nevirapine and 18. These results appear to confirm our hypothesis that a favorable effect of 3,5-difluorogenation, related to an attractive π -stacking interaction, takes place with the benzene rings of Tyr188. Also, it is consistent with the hypothesis that the presence of two electron-withdrawing groups at the meta positions of the phenyl ring would enhance the beneficial electronic effect on the antiviral activity produced by 3,5-difluorogenation.

The SI values of the major 16 derivatives for inhibiting HIV-1_{SF33} infection are in the range of 39 to 38 000. Strikingly, compound **7b**, which has the highest SI value, is highly effective against the NNRTI-resistant HIV-1 strain A17, suggesting great potential for further development as a new anti-HIV-1 drug.

EXPERIMENTAL SECTION

Chemistry. The structural characterization was performed with an NMR spectrometer and a high resolution mass spectrometer (HRMS).

The purity of tested compounds was determined by HPLC (Dionex Ultimate 3000 HPLC system). All the assayed compounds displayed a purity of ≥95% (Table S1, Supporting Information). Melting points were determined on a WBS-1B type digital melting-point apparatus and are uncorrected. NMR spectra were recorded on a Bruker Avance 300 or Avance 500 with tetramethylsilane (TMS) as an internal standard, and chemical shifts are reported in δ (ppm). All the reactions were routinely monitored by TLC, which was performed on aluminum-backed silica gel plates (60 F254) with spots visualized by UV light. Silica gel (0.040–0.064 mm) was used for column chromatography and analytical silica gel for TLC plates. Unless otherwise stated, all reagents were purchased from commercial sources. When necessary, they were purified and dried by standard methods. Organic solutions were dried over anhydrous sodium sulfate.

6-(Arylmethyl)-1-alkyl-5-halouracils 6a–9b. *General Procedure.* Activated zinc dust (18 g, 275 mmol) was suspended in dry THF (125 mL) at reflux, and a few drops of ethyl 2-bromoacetate were added to initiate the reaction. After the appearance of a green color (ca. 45 min), acrylonitrile (4.50 mmol) was added in one portion followed by dropwise addition of ethyl 2-bromoacetate (10 mmol) over a period of 1 h. The reaction mixture was refluxed for an additional 10 min, diluted with THF (3 × 125 mL), and quenched with aqueous K₂CO₃ (50%, 54 mL). Rapid stirring for 45 min gave two distinct layers. The upper layer was decanted, the residue was washed with THF (2 × 100 mL), and the combined THF fractions were treated with aqueous HCl (10%, 50 mL) at room temperature for 45 min. The mixture was concentrated in vacuo, diluted with CH₂Cl₂ (300 mL), and washed with saturated aqueous NaHCO₃ (200 mL) to pH 7. The organic phase was dried (Na₂SO₄) and evaporated in vacuo to give an oil, which was used without further purification for the synthesis of compound **2a–c**.

Sodium (2.2 g, 96 mmol) was dissolved in anhydrous EtOH (80 mL), and thiourea (5.2 g, 68 mmol) and compounds **1a–c** (4.5 mmol) were added to the clear solution. The reaction mixture was refluxed for 4 h and evaporated under reduced pressure until nearly dry, and the residue was redissolved in H₂O (50 mL). The 2-thiouracil was precipitated by acidification to pH 4 with 2 N aq HCl.

The precipitated 2-thiouracil was desulfurized by suspension in 10% aqueous chloroacetic acid (100 mL) and subsequent reflux for 24 h. After cooling to room temperature, the precipitate was filtered off, washed with cold EtOH and Et₂O, and finally dried in vacuo to give compounds **3a–c** as white solids.

6-Arylmethyluracil **3a–c** (0.5 mmol) was suspended in glacial HOAc (3 mL). Pb(OAc)₂ (0.22 mmol) was added in portions while stirring, followed by the addition of halogen (0.22 mmol). The suspension was stirred for 12 h at 50 °C and then diluted with H₂O

(120 mL). The precipitate was isolated, washed with H₂O, and dried in vacuo to give **4a–c**, **5a,b** as a solid product.

6-(Arylmethyl)-5-halouracil **4a–c** and **5a,b** (0.42 mmol) were dissolved in dry CHCl₃ (10 mL), and *N,O*-bis(trimethylsilyl)acetamide (BSA, 1.05 mmol) was added. After 30 min, the appropriate alkyl chloromethyl ether (0.51 mmol) and LiI (0.2 mmol) were added. The solution was stirred at room temperature for 4 h and then quenched with ice-cold sat. NaHCO₃ (25 mL). The aqueous phase was extracted with AcOEt (3 × 20 mL). The organic layer was dried with Na₂SO₄ and evaporated under reduced pressure. The residue was purified by silica column chromatography, giving the product.

6-Benzyl-1-ethoxymethyl-5-iodouracil (6a). white solid, yield 90%; mp 175–177 °C; ¹H NMR (300 MHz, DMSO-*d*₆) δ 1.22 (t, 3H, J = 6.9 Hz, CH₂CH₃), 3.64 (q, 2H, J = 6.9 Hz, OCH₂CH₃), 4.58 (s, 2H, CH₂Ph), 5.24 (s, 2H, NCH₂O), 7.14–7.28 (m, 5H, aryl), 9.26 (s, 1H, NH); ¹³C NMR (75 MHz, DMSO-*d*₆) δ: 15.01 (CH₂CH₃), 42.05 (CH₂Ph), 65.39 (OCH₂CH₃), 74.05 (NCH₂O), 79.17 (C-5), 127.48, 127.66, 129.38, 133.55 (aryl), 151.45 (C-6), 156.07 (C-2), 160.00 (C-4); *m/z* (ESI): HRMS (*m/z*) calcd for C₁₄H₁₅IN₂O₃ [M + H]⁺ 387.02001, found 387.02021.

6-(3,5-Dimethylbenzyl)-1-ethoxymethyl-5-iodouracil (6b). white solid, yield 89%; mp 177–178 °C; ¹H NMR (300 MHz, DMSO-*d*₆) δ 1.23 (t, 3H, J = 7.0 Hz, CH₂CH₃), 2.32 (s, 6H, 2CH₃), 3.65 (q, 2H, J = 7.0 Hz, OCH₂CH₃), 4.51 (s, 2H, CH₂Ar), 5.25 (s, 2H, NCH₂O), 6.79–6.96 (m, 3H, aryl), 9.29 (s, 1H, NH); ¹³C NMR (75 MHz, DMSO-*d*₆) δ: 15.06 (CH₂CH₃), 21.35 (CH₃Ar-C6), 41.92 (CH₂Ph), 65.39 (OCH₂CH₃), 74.05 (NCH₂O), 79.07 (C-5), 127.13, 127.66, 133.30, 139.08 (aryl), 151.52 (C-6), 156.33 (C-2), 160.13 (C-4); *m/z* (ESI): HRMS (*m/z*) calcd for C₁₆H₁₉IN₂O₃ [M + H]⁺ 415.05131, found 415.05181.

6-(3,5-Difluorobenzyl)-1-ethoxymethyl-5-iodouracil (6c). white solid, yield 70%; mp 198–200 °C; ¹H NMR (400 MHz, DMSO-*d*₆) δ 1.05 (t, 3H, J = 7.0 Hz, CH₂CH₃), 3.50 (q, 2H, J = 7.0 Hz, OCH₂CH₃), 3.97 (s, 2H, CH₂Ar), 5.19 (s, 2H, NCH₂O), 6.97–7.16 (m, 3H, aryl), 9.80 (s, 1H, NH); ¹³C NMR (100 MHz, DMSO-*d*₆) δ: 15.48 (CH₂CH₃), 41.82 (CH₂Ar), 65.17 (OCH₂CH₃), 71.26 (NCH₂O), 73.98 (C-5), 103.09, 112.32, 140.02, 164.15 (aryl), 151.39 (C-6), 153.39 (C-2), 161.29 (C-4); *m/z* (ESI): HRMS (*m/z*) calcd for C₁₄H₁₃F₂IN₂O₃ [M + H]⁺ 422.9939, found 423.00165.

6-Benzyl-1-benzyloxymethyl-5-iodouracil (7a). white solid, yield 89%; mp 165–166 °C; ¹H NMR (300 MHz, DMSO-*d*₆) δ 4.57 (s, 2H, CH₂Ph), 4.67 (s, 2H, OCH₂Ph), 5.32 (s, 2H, NCH₂O), 7.12–7.41 (m, 10H, aryl), 8.90 (s, 1H, NH); ¹³C NMR (75 MHz, DMSO-*d*₆) δ: 42.10 (CH₂Ph-C6), 72.11 (OCH₂Ph), 74.01 (NCH₂O), 79.14 (C-5), 127.47, 127.68, 127.84, 128.22, 128.56, 129.38, 133.46, 136.89 (aryl), 151.20 (C-6), 155.85 (C-2), 159.64 (C-4); *m/z* (ESI): HRMS (*m/z*) calcd for C₁₉H₁₇IN₂O₃ [M + H]⁺ 449.03566, found 449.03562.

1-Benzyloxymethyl-6-(3,5-dimethylbenzyl)-5-iodouracil (7b). white solid, yield 85%; mp 166–167 °C; ¹H NMR (300 MHz, DMSO-*d*₆) δ 2.31 (s, 6H, 2CH₃), 4.49 (s, 2H, CH₂Ar), 4.68 (s, 2H, OCH₂Ph), 5.33 (s, 2H, NCH₂O), 6.72–7.41 (m, 8H, aryl), 9.11 (s, 1H, NH); ¹³C NMR (75 MHz, DMSO-*d*₆) δ: 21.35 (CH₃Ar-C6), 41.99 (CH₂Ar-C6), 72.07 (OCH₂Ph), 74.00 (NCH₂O), 79.14 (C-5), 125.11, 127.03, 127.68, 127.88, 128.23, 128.58, 129.36, 133.21, 136.97, 139.08 (aryl), 151.41 (C-6), 156.11 (C-2), 159.93 (C-4); *m/z* (ESI): HRMS (*m/z*) calcd for C₂₁H₂₁IN₂O₃ [M + H]⁺ 477.06696, found 477.06701.

6-(3,5-Difluorobenzyl)-1-benzyloxymethyl-5-iodouracil (7c). white solid, yield 58%; mp 175–177 °C; ¹H NMR (400 MHz, DMSO-*d*₆) δ 4.46 (s, 2H, CH₂Ar), 4.61 (s, 2H, OCH₂Ph), 5.24 (s, 2H, NCH₂O), 6.72–7.34 (m, 8H, aryl), 9.86 (s, 1H, NH); ¹³C NMR (100 MHz, DMSO-*d*₆) δ: 41.66 (CH₂Ar-C6), 72.09 (OCH₂Ph), 74.01 (NCH₂O), 79.99 (C-5), 103.31, 110.46, 127.97, 128.35, 128.60, 136.66, 137.35, 164.71 (aryl), 151.46 (C-6), 154.31 (C-2), 162.22 (C-4); HRMS (*m/z*): calcd for C₁₉H₁₃F₂IN₂O₃ [M + H]⁺ 485.0095, found 485.01706.

6-Benzyl-5-bromo-1-ethoxymethyluracil (8a). white solid, yield 78%; mp 170–172 °C; ¹H NMR (300 MHz, DMSO-*d*₆) δ 1.21 (t, 3H, J = 6.9 Hz, CH₂CH₃), 3.62 (q, 2H, J = 6.9 Hz, OCH₂CH₃), 4.54 (s, 2H, CH₂Ph), 5.25 (s, 2H, NCH₂O), 7.21–7.96 (m, 5H, aryl), 9.36 (s,

1H, NH); ¹³C NMR (75 MHz, DMSO-*d*₆) δ: 15.03 (CH₂CH₃), 42.08 (CH₂Ph), 65.37 (OCH₂CH₃), 74.02 (NCH₂O), 101.9 (C-5), 127.47, 127.64, 129.39, 133.50 (aryl), 151.43 (C-6), 156.10 (C-2), 160.05 (C-4); HRMS (*m/z*): calcd for C₁₄H₁₅BrN₂O₃ [M + H]⁺ 339.03388, found 339.03409.

6-(3,5-Dimethylbenzyl)-5-bromo-1-ethoxymethyluracil (8b). white solid, yield 82%; mp 192–193 °C; ¹H NMR (500 MHz, DMSO-*d*₆) δ 1.24 (t, 3H, J = 7.0 Hz, CH₂CH₃), 2.32 (s, 6H, 2CH₃), 3.66 (q, 2H, J = 7.0 Hz, OCH₂CH₃), 4.41 (s, 2H, CH₂Ar), 5.23 (s, 2H, NCH₂O), 6.79–6.95 (m, 3H, aryl), 9.30 (s, 1H, NH); ¹³C NMR (125 MHz, DMSO-*d*₆) δ: 15.05 (CH₂CH₃), 21.33 (CH₃Ar-C6), 37.33 (CH₂Ar-C6), 65.40 (OCH₂CH₃), 73.74 (NCH₂O), 101.83 (C-5), 125.21, 129.33, 133.35, 139.08 (aryl), 151.07 (C-6), 153.44 (C-2), 158.91 (C-4); HRMS (*m/z*): calcd for C₁₆H₁₉BrN₂O₃ [M + H]⁺ 367.06518, found 367.06542.

6-Benzyl-1-benzyloxymethyl-5-bromouracil (9a). white solid, yield 80%; mp 168–170 °C; ¹H NMR (300 MHz, DMSO-*d*₆) δ 4.47 (s, 2H, CH₂Ph), 4.68 (s, 2H, OCH₂Ph), 5.56 (s, 2H, NCH₂O), 7.27–7.40 (m, 10H, aryl), 9.07 (s, 1H, NH); ¹³C NMR (75 MHz, DMSO-*d*₆) δ: 37.51 (CH₂Ph-C6), 72.11 (OCH₂Ph), 73.71 (NCH₂O), 101.97 (C-5), 127.54, 127.67, 127.85, 128.22, 128.56, 129.35, 133.54, 136.88 (aryl), 150.86 (C-6), 152.92 (C-2), 158.50 (C-4); HRMS (*m/z*): calcd for C₁₉H₁₇BrN₂O₃ [M + H]⁺ 401.04953, found 401.05027.

6-(3,5-Dimethylbenzyl)-1-benzyloxymethyl-5-bromouracil (9b). white solid, yield 78%; mp 157–159 °C; ¹H NMR (500 MHz, DMSO-*d*₆) δ 2.30 (s, 6H, 2CH₃), 4.39 (s, 2H, CH₂Ar), 4.69 (s, 2H, OCH₂Ph), 5.31 (s, 2H, NCH₂O), 6.72–7.41 (m, 8H, aryl), 9.39 (s, 1H, NH); ¹³C NMR (125 MHz, DMSO-*d*₆) δ: 21.32 (CH₃Ar-C6), 37.37 (CH₂Ar-C6), 72.07 (OCH₂Ph), 73.68 (NCH₂O), 101.92 (C-5), 125.19, 127.77, 127.82, 127.90, 128.46, 128.58, 129.36, 133.28, 136.94, 139.07 (aryl), 151.04 (C-6), 153.20 (C-2), 158.83 (C-4); HRMS (*m/z*): calcd for C₂₁H₂₁BrN₂O₃ [M + H]⁺ 429.08083, found 429.08150.

6-(Arylmethyl)-1-alkyl-5-dimethylaminouracils 10a,b, 11a,b. *General Procedure*. A mixture of 1-alkyl-6-(arylmethyl)-5-iodouracil (0.2 mmol), 33% aqueous NH(CH₃)₂ solution (2.4 mL), and 1,4-dioxane (2.4 mL) was reacted in a high-pressure reactor at 80 °C for 1 h. After cooling to room temperature, the reaction mixture was extracted with CH₂Cl₂ (2 × 25 mL). The combined organic layer was dried with Na₂SO₄ and evaporated under reduced pressure. The residue was purified by silica column chromatography, giving the products.

6-Benzyl-5-dimethylamino-1-ethoxymethyluracil (10a). white solid, yield 58%; mp 80–81 °C; ¹H NMR (500 MHz, DMSO-*d*₆) δ 1.21 (t, 3H, J = 7.0 Hz, CH₂CH₃), 2.73 (s, 6H, N(CH₃)₂), 3.62 (q, 2H, J = 7.0 Hz, OCH₂CH₃), 4.43 (s, 2H, CH₂Ph), 5.10 (s, 2H, NCH₂O), 7.14–7.36 (m, 5H, aryl), 9.44 (s, 1H, NH); ¹³C NMR (125 MHz, DMSO-*d*₆) δ: 15.06 (CH₂CH₃), 32.28 (CH₂Ph-C6), 43.64 (N(CH₃)₂), 65.02 (OCH₂CH₃), 73.17 (NCH₂O), 126.75 (C-5), 126.88, 127.47, 136.18, 138.66 (aryl), 151.68 (C-6), 152.85 (C-2), 161.42 (C-4); HRMS (*m/z*): calcd for C₁₆H₂₁N₃O₃ [M + H]⁺ 304.16557, found 304.16521.

6-(3,5-Dimethylbenzyl)-5-dimethylamino-1-ethoxymethyluracil (10b). white solid, yield 50%; mp 171–173 °C; ¹H NMR (500 MHz, DMSO-*d*₆) δ 1.22 (t, 3H, J = 7.1 Hz, CH₂CH₃), 2.31 (s, 6H, CH₃Ph), 2.75 (s, 6H, N(CH₃)₂), 3.42 (q, 2H, J = 7.1 Hz, OCH₂CH₃), 4.36 (s, 2H, CH₂Ar), 5.11 (s, 2H, NCH₂O), 6.73–6.90 (m, 3H, aryl), 8.96 (s, 1H, NH); ¹³C NMR (125 MHz, DMSO-*d*₆) δ: 15.06 (CH₂CH₃), 21.29 (CH₃Ar-C6), 32.11 (CH₂Ar-C6), 43.66 (N(CH₃)₂), 65.02 (OCH₂CH₃), 73.17 (NCH₂O), 126.52 (C-5), 125.21, 128.52, 136.18, 138.66 (aryl), 151.47 (C-6), 153.16 (C-2), 161.11 (C-4); HRMS (*m/z*): calcd for C₁₈H₂₃N₃O₃ [M + H]⁺ 332.19687, found 332.19622.

6-Benzyl-1-benzyloxymethyl-5-dimethylaminouracil (11a). white solid, yield 56%; mp 91–92 °C; ¹H NMR (500 MHz, DMSO-*d*₆) δ 2.72 (s, 6H, N(CH₃)₂), 4.43 (s, 2H, CH₂Ph), 4.67 (s, 2H, OCH₂Ph), 5.21 (s, 2H, NCH₂O), 7.25–7.39 (m, 10H, aryl), 9.17 (s, 1H, NH); ¹³C NMR (125 MHz, DMSO-*d*₆) δ: 32.27 (CH₂Ph-C6), 43.64 (N(CH₃)₂), 71.94 (OCH₂Ph), 73.29 (NCH₂O), 126.76 (C-5), 126.92, 127.47, 127.77, 128.03, 128.35, 128.52, 129.10, 136.34, 137.39 (aryl), 151.68 (C-6), 152.64 (C-2), 161.12 (C-4); HRMS (*m/z*): calcd for C₂₁H₂₃N₃O₃ [M + H]⁺ 366.18122, found 366.18047.

6-(3,5-Dimethylbenzyl)-1-benzyloxymethyl-5-dimethylaminouracil (11b). white solid, yield 51%; mp 152–153 °C; $^1\text{H NMR}$ (300 MHz, DMSO- d_6) δ 2.28 (s, 6H, CH_3Ph), 2.72 (s, 6H, $\text{N}(\text{CH}_3)_2$), 4.34 (s, 2H, CH_2Ar), 4.67 (s, 2H, OCH_2Ph), 5.20 (s, 2H, NCH_2O), 6.70–7.39 (m, 8H, aryl), 9.10 (s, 1H, NH); $^{13}\text{C NMR}$ (75 MHz, DMSO- d_6) δ : 21.29 (CH_3Ar), 32.07 ($\text{CH}_2\text{Ar-C6}$), 43.62 ($\text{N}(\text{CH}_3)_2$), 71.90 (OCH_2Ph), 73.31 (NCH_2O), 126.61 (C-5), 125.19, 127.47, 128.00, 128.35, 128.49, 136.07, 137.44, 138.65 (aryl), 151.68 (C-6), 152.64 (C-2), 161.12 (C-4); HRMS (m/z): calcd for $\text{C}_{23}\text{H}_{27}\text{N}_3\text{O}_3$ [$\text{M} + \text{H}$] $^+$ 394.21252, found 394.21203.

4-Amino-6-(arylmethyl)-1-alkyl-5-halouracils 12a,b, 13a,b, 14a,b, 15a,b. *General Procedure.* 1-Alkyl-6-arylmethyl-5-halouracil (0.067 mmol) was added to the solution of 1,2,4-triazole (1.34 mmol) and POCl_3 (0.53 mmol) in the presence of triethylamine. After being stirred for about 30 min, the solution became dark-red. Concentrated ammonia (1 mL, 25–28%) was added dropwise to the mixture and reacted for another 1 h. The reaction mixture was extracted with dichloromethane, and the combined organic layer was dried with Na_2SO_4 and evaporated in vacuo. The residue was purified by silica column chromatography to yield the products.

4-Amino-6-benzyl-1-ethoxymethyl-5-iodouracil (12a). white solid, yield 46%; mp 150–152 °C; $^1\text{H NMR}$ (300 MHz, DMSO- d_6) δ 1.12 (t, 3H, $J = 6.9$ Hz, CH_2CH_3), 3.46 (q, 2H, $J = 6.9$ Hz, OCH_2CH_3), 4.38 (s, 2H, CH_2Ph), 5.17 (s, 2H, NCH_2O), 7.12–7.37 (m, 5H, Ph), 8.23 (br, 2H, $\text{NH}_2\text{-C4}$); $^{13}\text{C NMR}$ (75 MHz, DMSO- d_6) δ : 15.33 (CH_2CH_3), 41.98 (CH_2Ph), 64.26 (OCH_2CH_3), 67.60 (NCH_2O), 74.21 (C-5), 127.32, 127.83, 129.41, 133.22 (aryl), 151.16 (C-6), 156.89 (C-2), 164.75 (C-4); m/z (ESI): 386.2 ($\text{M} + \text{H}$) $^+$.

4-Amino-6-(3,5-dimethylbenzyl)-1-ethoxymethyl-5-iodouracil (12b). white solid, yield 78%; mp 113–115 °C; $^1\text{H NMR}$ (300 MHz, DMSO- d_6) δ 1.04 (t, 3H, $J = 7.0$ Hz, CH_2CH_3), 2.24 (s, 6H, 2CH_3), 3.49 (q, 2H, $J = 7.0$ Hz, OCH_2CH_3), 4.31 (s, 2H, CH_2Ar), 5.17 (s, 2H, NCH_2O), 6.73–6.89 (m, 3H, aryl), 8.49 (br, 2H, $\text{NH}_2\text{-C4}$); $^{13}\text{C NMR}$ (75 MHz, DMSO- d_6) δ : 15.32 (OCH_2CH_3), 21.37 ($\text{CH}_3\text{Ar-C6}$), 41.66 ($\text{CH}_2\text{Ar-C6}$), 64.33 (OCH_2CH_3), 67.55 (NCH_2O), 74.26 (C-5), 125.44, 128.86, 135.01, 138.48 (aryl), 156.28 (C-6), 157.05 (C-2), 164.75 (C-4); m/z (ESI): 414.3 ($\text{M} + \text{H}$) $^+$.

4-Amino-6-benzyl-1-benzyloxymethyl-5-iodouracil (13a). white solid, yield 58%; mp 138–139 °C; $^1\text{H NMR}$ (500 MHz, DMSO- d_6) δ 4.39 (s, 2H, CH_2Ph), 4.55 (s, 2H, OCH_2Ph), 5.25 (s, 2H, NCH_2O), 7.09–7.34 (m, 10H, aryl), 7.98 (br, 2H, $\text{NH}_2\text{-C4}$); $^{13}\text{C NMR}$ (125 MHz, DMSO- d_6) δ : 41.85 ($\text{CH}_2\text{Ph-C6}$), 67.61 (OCH_2Ph), 70.80 (NCH_2O), 74.41 (C-5), 127.35, 127.87, 128.06, 128.13, 128.70, 129.43, 135.13, 138.12 (aryl), 156.14 (C-6), 156.85 (C-2), 164.80 (C-4); m/z (ESI): 448.3 ($\text{M} + \text{H}$) $^+$.

4-Amino-1-benzyloxymethyl-6-(3,5-dimethylbenzyl)-5-iodouracil (13b). white solid, yield 58%; mp 129–130 °C; $^1\text{H NMR}$ (500 MHz, DMSO- d_6) δ 2.21 (s, 6H, 2CH_3), 4.29 (s, 2H, CH_2Ar), 4.55 (s, 2H, OCH_2Ph), 5.23 (s, 2H, NCH_2O), 6.70–7.36 (m, 8H, aryl), 8.60 (br, 2H, $\text{NH}_2\text{-C4}$); $^{13}\text{C NMR}$ (125 MHz, DMSO- d_6) δ : 21.37 ($\text{CH}_3\text{Ar-C6}$), 41.89 ($\text{CH}_2\text{Ar-C6}$), 68.06 (OCH_2Ph), 72.30 (NCH_2O), 78.04 (C-5), 126.11, 127.30, 127.86, 128.08, 128.32, 128.68, 129.40, 133.27, 136.97, 139.18 (aryl), 152.41 (C-6), 155.01 (C-2), 160.03 (C-4); m/z (ESI): 476.4 ($\text{M} + \text{H}$) $^+$.

4-Amino-6-benzyl-5-bromo-1-ethoxymethyluracil (14a). white solid, yield 48%; mp decomposed >200 °C; $^1\text{H NMR}$ (500 MHz, DMSO- d_6) δ 1.05 (t, 3H, $J = 6.9$ Hz, CH_2CH_3), 3.58 (q, 2H, $J = 6.9$ Hz, OCH_2CH_3), 4.46 (s, 2H, CH_2Ph), 5.23 (s, 2H, NCH_2O), 7.151–7.87 (m, 5H, aryl), 8.30 (br, 2H, $\text{NH}_2\text{-C4}$); $^{13}\text{C NMR}$ (125 MHz, DMSO- d_6) δ : 15.07 (CH_2CH_3), 41.96 (CH_2Ph), 64.73 (OCH_2CH_3), 74.01 (NCH_2O), 90.89 (C-5), 125.67, 128.14, 133.39, 139.50 (aryl), 152.43 (C-6), 157.01 (C-2), 159.05 (C-4); m/z (ESI): 338.3, 340.2 ($\text{M} + \text{H}$) $^+$.

4-Amino-6-(3,5-dimethylbenzyl)-5-bromo-1-ethoxymethyluracil (14b). white solid, yield 91%; mp 111–112 °C; $^1\text{H NMR}$ (500 MHz, DMSO- d_6) δ 1.04 (t, 3H, $J = 7.0$ Hz, CH_2CH_3), 2.24 (s, 6H, $2\text{CH}_3\text{Ph}$), 3.50 (q, 2H, $J = 7.0$ Hz, OCH_2CH_3), 4.22 (s, 2H, CH_2Ar), 5.15 (s, 2H, NCH_2O), 6.74–6.89 (m, 3H, aryl), 8.40 (br, 2H, $\text{NH}_2\text{-C4}$); $^{13}\text{C NMR}$ (125 MHz, DMSO- d_6) δ : 15.31 (OCH_2CH_3), 21.35

($\text{CH}_3\text{Ar-C6}$), 37.22 ($\text{CH}_2\text{Ar-C6}$), 64.32 (OCH_2CH_3), 74.08 (NCH_2O), 91.68 (C-5), 125.48, 128.89, 134.99, 138.48 (aryl), 154.14 (C-6), 155.67 (C-2), 162.66 (C-4); m/z (ESI): 366.3 ($\text{M} + \text{H}$) $^+$.

4-Amino-6-benzyl-1-benzyloxymethyl-5-bromouracil (15a). yield 60%; mp 148–149 °C; $^1\text{H NMR}$ (500 MHz, DMSO- d_6) δ 4.30 (s, 2H, CH_2Ph), 4.55 (s, 2H, OCH_2Ph), 5.24 (s, 2H, NCH_2O), 7.11–7.34 (m, 10H, aryl), 8.00 (br, 2H, $\text{NH}_2\text{-C4}$); $^{13}\text{C NMR}$ (125 MHz, DMSO- d_6) δ : 37.39 ($\text{CH}_2\text{Ph-C6}$), 70.77 (OCH_2Ph), 74.17 (NCH_2O), 91.86 (C-5), 127.41, 127.89, 128.09, 128.17, 128.70, 129.44, 135.05, 138.07 (aryl), 153.94 (C-6), 155.59 (C-2), 162.69 (C-4); m/z (ESI): 400.3, 402.2 ($\text{M} + \text{H}$) $^+$.

4-Amino-1-benzyloxymethyl-6-(3,5-dimethylbenzyl)-5-bromouracil (15b). white solid, yield 84%; mp 137–138 °C; $^1\text{H NMR}$ (500 MHz, DMSO- d_6) δ 2.19 (s, 6H, 2CH_3), 4.27 (s, 2H, CH_2Ar), 4.60 (s, 2H, OCH_2Ph), 5.32 (s, 2H, NCH_2O), 6.69–7.43 (m, 8H, aryl), 7.89 (br, 2H, $\text{NH}_2\text{-C4}$); $^{13}\text{C NMR}$ (125 MHz, DMSO- d_6) δ : 21.22 ($\text{CH}_3\text{Ar-C6}$), 41.70 ($\text{CH}_2\text{Ar-C6}$), 71.98 (OCH_2Ph), 74.20 (NCH_2O), 87.14 (C-5), 126.34, 127.5, 127.96, 128.18, 128.45, 128.87, 129.65, 133.43, 137.07, 140.09 (aryl), 153.47 (C-6), 156.14 (C-2), 163.23 (C-4); m/z (ESI): 428.4 ($\text{M} + \text{H}$) $^+$.

Biological Assays. *Assay for Measuring the Inhibitory Activity of Compounds against HIV-1 RT.* Oligo(dT) (TaKaRa Co., Japan) was immobilized via its 5'-terminal phosphate to Covalink-NH microtiter plates (NUNC Co., Denmark). The biotin-dUTP was incorporated by reverse transcriptase (Sigma). Briefly, a serial concentration of inhibitor was added to the mixture, which contained 50 mmol/L Tris-HCl (pH 8.3), 3 mmol/L MgCl_2 , 75 mmol/L KCl, 5 mmol/L DTT (D,L -dithiothreitol), 0.13 mg/mL BSA (Albumin Bovine V), 10 μM mL poly (A), 0.75 μM biotin-11-dUTP, and 1.5 μM dTTP. The reaction mixture was incubated at 37 °C for 1 h and washed with a buffer containing 50 mmol/L Tris-HCl (pH 7.5), 0.15 mol/L NaCl, 0.05 mmol/L MgCl_2 , and 0.02% Tween-20. After 100 μL of 1% BSA was added to each well and incubated at room temperature for another 30 min, the plate was washed with the same buffer. Before further incubation at 37 °C for 1 h, 50 μL of SA-ALP (alkaline phosphatase streptavidin) solution (100 ng/mL) was added to each well, and the plate was washed again as above. Finally, 50 μL of PNPP (*p*-nitrophenyl phosphate, disodium) (1 mg/mL, pH 9.5) was added and incubated at 37 °C for 30 min. The reaction was stopped by addition of 0.5 M NaOH. The inhibitory activity of the compounds was detected and quantified using a colorimetric streptavidin-alkaline phosphatase reporter system.

Assay for Measuring the Inhibitory Activity of Compounds on HIV-1_{SF33} and HIV-1_{A17} Replication in MT4. MT4 cells, HIV-1_{SF33}, HIV-1_{IIIB}, and HIV-1_{A17} were obtained from the NIH AIDS Research and Reference Reagent Program (Germantown, MD). The inhibitory activity of the compounds on infection by a laboratory-adapted HIV-1 strain SF33 and an NNRTI-resistant HIV-1 strain A17 was tested in MT4 cells. Briefly, MT4 cells (4×10^4 /well) were infected by addition of 200 TCID₅₀ of HIV-1, followed by incubation for 2 h at 37 °C before addition of compounds at serial dilutions. After further incubation at 37 °C for 7 days, p24 was measured using a commercial enzyme-linked immunosorbent assay (ELISA) kit (Vironostika HIV-1 Microelisa system; BioMérieux; Marcy l'Etoile, France). The concentration of a compound for inhibiting 50% viral replication (EC_{50}) was determined by nonlinear regression using GraphPad Prism 5.01.

Assessment of in Vitro Cytotoxicity in MT-4 Cell. An XTT assay, as previously described,³³ was used to assess the cytotoxicity of target compounds to MT4 cells. Briefly, a compound at graded concentrations was added to MT4 cells (5×10^4 /well), followed by an incubation at 37 °C for 3 days. Ten microliters of CCK-8 reagent was added to the cells. After incubation at 37 °C for 4 h to allow color development of the XTT formazan product, the absorbance of each well was then read at 450 nm in a Victor2 1420 Multilabel Counter (Wallace-PerkinElmer Life and Analytical Sciences Inc., Boston, MA). The percent of cytotoxicity and CC_{50} (concentration causing 50% cytotoxicity) were calculated as previously described.³⁷

Molecular Modeling. The docking studies were conducted by using software GOLD3.0.1 and two protein crystal structures of wild-type RT/1 complex (PDB ID: 1RT2) and Y181C mutant RT/2 complex (PDB: 1JLA). Following the default setting of Chemscore in the software tool, top scored docked poses were visually inspected for each ligand in the DS 2.5 based on relevant molecules. The radius of the binding site sphere was defined by the original ligand as 8.9 Å, thus ensuring that the docking method was reliable.

■ ASSOCIATED CONTENT

● Supporting Information

Additional information as noted in the text. This material is available free of charge via the Internet at <http://pubs.acs.org>.

■ AUTHOR INFORMATION

Corresponding Author

*Phone/fax: +86-10-82805203, e-mail: jyliu@bjmu.edu.cn (J.L.); or phone: +86-10-58900976, fax: +86-10-58900980, e-mail: mal@chinaaids.cn (L.M.).

Author Contributions

[#]These authors have contributed equally.

Notes

The authors declare no competing financial interest.

■ ACKNOWLEDGMENTS

We thank the NIH AIDS Research and Reference Reagent Program in the USA for providing MT4 cells, HIV-1_{5F33}, and HIV-1_{A17}. This study was supported by the National Science Foundation of China (20972011, 21042009, 21172014, 30872232, and 81172733) and grants from the Ministry of Science and Technology of China (2009ZX09301-010) and SKLID development grant (2011SKLID102) for financial support.

■ ABBREVIATIONS USED

CC₅₀, concentration for 50% cytotoxicity; EC₅₀, effective concentration for 50% inhibition; ELISA, enzyme-linked immunosorbent assay; HAART, highly active antiretroviral therapy; HIV-1, human immunodeficiency virus type 1; HEPT, (1-[2-hydroxyethoxymethyl]-6-(phenylthio)thymine]; NNBP, non-nucleoside binding pocket; NNIBP, the non-nucleoside inhibitor binding pocket; NNRTI, non-nucleoside reverse transcriptase inhibitor; PDB, protein database; RT, reverse transcriptase; RTI, reverse transcriptase inhibitor; SI, selectivity index (ratio of CC₅₀/EC₅₀)

■ REFERENCES

- (1) Tronchet, J. M.; Seman, M. Nonnucleoside inhibitors of HIV-1 reverse transcriptase: from the biology of reverse transcription to molecular design. *Curr. Top. Med. Chem.* **2003**, *3*, 1496–1511.
- (2) Tarby, C. M. Recent advances in the development of next generation non-nucleoside reverse transcriptase inhibitors. *Curr. Top. Med. Chem.* **2004**, *4*, 1045–1057.
- (3) Sluis-Cremer, N.; Temiz, N. A.; Bahar, I. Conformational changes in HIV-1 reverse transcriptase induced by nonnucleoside reverse transcriptase inhibitor binding. *Curr. HIV Res.* **2004**, *2*, 323–332.
- (4) De Clercq, E. New developments in anti-HIV chemotherapy. *Biochim. Biophys. Acta* **2002**, *1587*, 258–275.
- (5) Ren, J.; Esnouf, R.; Garman, E.; Somers, D.; Ross, C.; Kirby, I.; Keeling, J.; Darby, G.; Jones, Y.; Stuart, D.; Stammers, D. High resolution structures of HIV-1 RT from four RT-inhibitor complexes. *Nat. Struct. Biol.* **1995**, *2*, 293–302.

- (6) Esnouf, R.; Ren, J.; Ross, C.; Jones, Y.; Stammers, D.; Stuart, D. Mechanism of inhibition of HIV-1 reverse transcriptase by nonnucleoside inhibitors. *Nat. Struct. Biol.* **1995**, *2*, 303–308.

- (7) Smerdon, S. J.; Jager, J.; Wang, J.; Kohlstaedt, L. A.; Chirino, A. J.; Friedman, J. M.; Rice, P. A.; Steitz, T. A. Structure of the binding site for nonnucleoside inhibitors of the reverse transcriptase of human immunodeficiency virus type 1. *Proc. Natl. Acad. Sci. U.S.A.* **1994**, *91*, 3911–3915.

- (8) Jonckheere, H.; Anne, J.; De Clercq, E. The HIV-1 reverse transcription (RT) process as target for RT inhibitors. *Med. Res. Rev.* **2000**, *20*, 129–154.

- (9) Das, K.; Clark, A. D. Jr.; Lewi, P. J.; Heeres, J.; de Jonge, M. R.; Koymans, L. M. H.; Vinkers, H. M.; Daeyaert, F.; Ludovici, D. W.; Kukla, M. J.; De Corte, B.; Kavash, R. W.; Ho, C. Y.; Ye, H.; Lichtenstein, M. A.; Andries, K.; Pauwels, R.; de Bethune, M.-P.; Boyer, P. L.; Clark, P.; Hughes, S. H.; Janssen, P. A. J.; Arnold, E. Roles of Conformational and positional adaptability in structure-based design of TMC125-R165335 (etravirine) and related non-nucleoside reverse transcriptase inhibitors that are highly potent and effective against wild-type and drug-resistant HIV-1 variants. *J. Med. Chem.* **2004**, *47*, 2550–2560.

- (10) Ding, J.; Das, K.; Tantillo, C.; Zhang, W.; Clark, A. J.; Jessen, S.; Lu, X.; Hsiou, Y.; Jacobo-Molina, A.; Andries, K.; Et, A. Structure of HIV-1 reverse transcriptase in a complex with the non-nucleoside inhibitor alpha-APA R 95845 at 2.8 Å resolution. *Structure* **1995**, *3*, 365–379.

- (11) Ding, J.; Das, K.; Moereels, H.; Koymans, L.; Andries, K.; Janssen, P. A.; Hughes, S. H.; Arnold, E. Structure of HIV-1 RT/TIBO R 86183 complex reveals similarity in the binding of diverse nonnucleoside inhibitors. *Nat. Struct. Biol.* **1995**, *2*, 407–415.

- (12) Esnouf, R. M.; Stuart, D. I.; De Clercq, E.; Schwartz, E.; Balzarini, J. Models which explain the inhibition of reverse transcriptase by HIV-1-specific (thio)carboxanilide derivatives. *Biochem. Biophys. Res. Commun.* **1997**, *234*, 458–464.

- (13) Coffin, J. M. HIV population dynamics in vivo: implications for genetic variation, pathogenesis, and therapy. *Science* **1995**, *267*, 483–489.

- (14) Ma, L.; Huang, J.; Xing, H.; Yuan, L.; Yu, X.; Sun, J.; Huang, Y.; Qu, S.; Feng, Y.; Liao, L.; Liu, S.; Shao, Y. Genotypic and phenotypic cross-drug resistance of harboring drug-resistant HIV type 1 subtype B' strains from former blood donors in central Chinese provinces. *AIDS Res. Hum. Retroviruses* **2010**, *26*, 1007–1013.10. Arnold, E.; Das, K.; Ding, J.; Yadav, P. N.; Hsiou, Y.; Boyer, P. L.; Hughes, S. H. Targeting HIV reverse transcriptase for anti-AIDS drug design: structural and biological considerations for chemotherapeutic strategies. *Drug Des. Discovery* **1996**, *13*, 29–47.

- (15) Ren, J.; Stammers, D. K. HIV reverse transcriptase structures: designing new inhibitors and understanding mechanisms of drug resistance. *Trends Pharmacol. Sci.* **2005**, *26*, 4–7.

- (16) Das, K.; Lewi, P. J.; Hughes, S. H.; Arnold, E. Crystallography and the design of anti-AIDS drugs: conformational flexibility and positional adaptability are important in the design of non-nucleoside HIV-1 reverse transcriptase inhibitors. *Prog. Biophys. Mol. Biol.* **2005**, *88*, 209–231.

- (17) Ma, L.; Sun, J.; Xing, H.; Si, X.; Yuan, L.; Guo, Y.; Cheng, H.; Shao, Y. Genotype and phenotype patterns of drug-resistant HIV-1 subtype B' (Thai B) isolated from patients failing antiretroviral therapy in China. *J. Acquired Immune Defic. Syndr.* **2007**, *44*, 14–19.

- (18) Baba, M.; De Clercq, E.; Tanaka, H.; Ubasawa, M.; Takashima, H.; Sekiya, K.; Nitta, I.; Umez, K.; Nakashima, H.; Mori, S.; Et, A. Potent and selective inhibition of human immunodeficiency virus type 1 (HIV-1) by 5-ethyl-6-phenylthiouracil derivatives through their interaction with the HIV-1 reverse transcriptase. *Proc. Natl. Acad. Sci. U.S.A.* **1991**, *88*, 2356–2360.

- (19) Campiani, G.; Ramunno, A.; Maga, G.; Nacci, V.; Fattorusso, C.; Catalanotti, B.; Morelli, E.; Novellino, E. Non-nucleoside HIV-1 reverse transcriptase (RT) inhibitors: past, present, and future perspectives. *Curr. Pharm. Des.* **2002**, *8*, 615–657.

- (20) Baba, M.; Tanaka, H.; Miyasaka, T.; Yuasa, S.; Ubasawa, M.; Walker, R. T.; De Clercq, E. Hept derivatives: 6-Benzyl-1-ethoxymethyl-5-isopropyluracil (MKC-442). *Nucleosides Nucleotides* **1995**, *14*, 575–583.
- (21) Sankatsing, S. U.; Weverling, G. J.; Peeters, M.; Van't, K. G.; Gruzdev, B.; Rakhmanova, A.; Danner, S. A.; Jurriaans, S.; Prins, J. M.; Lange, J. M. TMC125 exerts similar initial antiviral potency as a five-drug, triple class antiretroviral regimen. *AIDS* **2003**, *17*, 2623–2627.
- (22) Hopkins, A. L.; Ren, J.; Esnouf, R. M.; Willcox, B. E.; Jones, E. Y.; Ross, C.; Miyasaka, T.; Walker, R. T.; Tanaka, H.; Stammers, D. K.; Stuart, D. I. Complexes of HIV-1 reverse transcriptase with inhibitors of the HEPT series reveal conformational changes relevant to the design of potent non-nucleoside inhibitors. *J. Med. Chem.* **1996**, *39*, 1589–1600.
- (23) Kireev, D. B.; Chretien, J. R.; Grierson, D. S.; Monneret, C. A 3D QSAR study of a series of HEPT analogues: the influence of conformational mobility on HIV-1 reverse transcriptase inhibition. *J. Med. Chem.* **1997**, *40*, 4257–4264.
- (24) Esnouf, R. M.; Ren, J.; Hopkins, A. L.; Ross, C. K.; Jones, E. Y.; Stammers, D. K.; Stuart, D. I. Unique features in the structure of the complex between HIV-1 reverse transcriptase and the bis(heteroaryl)-piperazine (BHAP) U-90152 explain resistance mutations for this nonnucleoside inhibitor. *Proc. Natl. Acad. Sci. U.S.A.* **1997**, *94*, 3984–3989.
- (25) Mai, A.; Artico, M.; Sbardella, G.; Massa, S.; Novellino, E.; Greco, G.; Loi, A. G.; Tramontano, E.; Marongiu, M. E.; La Colla, P. 5-Alkyl-2-(alkylthio)-6-(2,6-dihalophenylmethyl)-3,4-dihydropyrimidin-4(3H)-ones: novel potent and selective dihydro-alkoxy-benzyl-oxopyrimidine derivatives. *J. Med. Chem.* **1999**, *42*, 619–627.
- (26) Hannick, S. M.; Kishi, Y. An improved procedure for the Blaise reaction: a short, practical route to the key intermediates of the saxitoxin synthesis. *J. Org. Chem.* **1983**, *48*, 3833–3835.
- (27) Danel, K.; Larsen, E.; Pedersen, E. B. Easy synthesis of 5,6-disubstituted acyclouridine derivatives. *Synthesis* **1995**, *8*, 934–936.
- (28) Petersen, L.; Pedersen, E. B.; Nielsen, C. Three routes for the synthesis of 6-benzyl-1-ethoxymethyl-2,4-dioxo-1,2,3,4-tetrahydropyrimidine-5-carbaldehyde. *Synthesis* **2001**, *4*, 559–564.
- (29) Wamberg, M.; Pedersen, E. B.; Nielsen, C. Synthesis of furoannelated analogues of Emivirine (MKC-442). *Arch. Pharm. (Weinheim)* **2004**, *337*, 148–151.
- (30) Danel, K.; Larsen, E.; Pedersen, E. B.; Vestergaard, B. F.; Nielsen, C. Synthesis and potent anti-HIV-1 activity of novel 6-benzyluracil analogues of 1-[(2-hydroxyethoxy)methyl]-6-(phenylthio)thymine. *J. Med. Chem.* **1996**, *39*, 2427–2431.
- (31) Muller, C. E.; Thorand, M.; Qurishi, R.; Diekmann, M.; Jacobson, K. A.; Padgett, W. L.; Daly, J. W. Imidazo[2,1-*i*]purin-5-ones and related tricyclic water-soluble purine derivatives: potent A(2A)- and A(3)-adenosine receptor antagonists. *J. Med. Chem.* **2002**, *45*, 3440–3450.
- (32) Elderfield, R.; Jesse, W. Application of the Mannich reaction with β,β -dichlorodiethylamine to derivatives of uracil. *J. Org. Chem.* **1961**, *26*, 3042–3043.
- (33) Sung, W. L. Synthesis of 4-(1,2,4-triazol-1-yl)-pyrimidin-2(1H)-one ribonucleotide and its application in synthesis of oligoribonucleotides. *J. Org. Chem.* **1982**, *47*, 3623–3628.
- (34) Lavandera, I.; Fernández, S.; M., F.; Gotor, V. Novel and efficient syntheses of 3',5'-diamino derivatives of 2',3',5'-trideoxycytidine and 2',3',5'-trideoxyadenosine. Protonation behavior of 3',5'-diaminonucleosides. *Tetrahedron* **2003**, *59*, 5449–5456.
- (35) Evelina, C.; Antonella, C.; Liguori, A.; Napoli, A.; Siciliano, C.; Sindona, G. Simple and efficient routes for the preparation of isoxazolidinyl nucleosides containing cytosine and 5-methyl-cytosine as new potential anti-HIV drugs. *Tetrahedron* **2001**, *57*, 8551–8557.
- (36) Lu, X.; Chen, Y.; Guo, Y.; Liu, Z.; Shi, Y.; Xu, Y.; Wang, X.; Zhang, Z.; Liu, J. The design and synthesis of N-1-alkylated-5-aminoarylalkylsubstituted-6-methyluracils as potential non-nucleoside HIV-1 RT inhibitors. *Bioorg. Med. Chem.* **2007**, *15*, 7399–7407.
- (37) Jiang, S.; Lu, H.; Liu, S.; Zhao, Q.; He, Y.; Debnath, A. K. N-substituted pyrrole derivatives as novel human immunodeficiency virus type 1 entry inhibitors that interfere with the gp41 six-helix bundle formation and block virus fusion. *Antimicrob. Agents Chemother.* **2004**, *48*, 4349–4359.